ELSEVIER

https://www.jhltopen.org/

Hyperpolarized ^{129}Xe MRI and spectroscopy of gas-exchange abnormalities in bilateral lung transplant recipients

Austin Simmons, MS,[a] David Mummy, PhD,[b] Shuo Zhang, PhD,[b] Suphachart Leewiwatwong, BS,[b] Scott Palmer, MD,[c] Bastiaan Driehuys, PhD,[b,d,e] and Hakim Azfar Ali, MD[c,*]

[a]*Campbell University School of Osteopathic Medicine, Buies Creek, North Carolina*
[b]*Department of Radiology, Duke University, Durham, North Carolina*
[c]*Department of Medicine, Duke University, Durham, North Carolina*
[d]*Department of Biomedical Engineering, Duke University, Durham, North Carolina*
[e]*Department of Medical Physics, Duke University, Durham, North Carolina*

KEYWORDS:
lung transplant;
CLAD;
functional lung imaging;
129Xe MRI;
spectroscopy

BACKGROUND: There is currently no sensitive, noninvasive method of screening for chronic lung allograft dysfunction (CLAD), the primary barrier to long-term survival after lung transplant. Conventional pulmonary function testing is imprecise absent a sustained decline. Hyperpolarized ^{129}Xe magnetic resonance imaging (MRI) is a sensitive tool for 3-dimensional imaging of regional pulmonary ventilation and gas-exchange abnormalities and may aid in early detection of CLAD.

METHODS: Adult patients, post bilateral lung transplant, were screened for CLAD based on the International Society for Heart and Lung Transplantation criteria. Those with established allografts (n = 10) underwent ^{129}Xe gas-exchange MRI and spectroscopy and were compared to results from 16 young healthy volunteers and 16 age-matched healthy volunteers. One lung transplant recipient was excluded from the final data analysis due to a concurrent lung infection found incidentally after MRI. Imaging provided quantitative maps of the ventilation defect percent (VDP), membrane high percent, and red blood cell (RBC) defect percent. Spectroscopy yielded RBC/membrane ratio, oxygenation-dependent RBC shift, and RBC oscillation amplitude.

RESULTS: The analysis included 9 lung transplant recipients, 7 with CLAD and 2 without. CLAD patients exhibited VDP values consistent with their forced expiratory volume in 1 second (FEV_1) decline (rho = 0.79, p = 0.048). Hemoglobin-corrected RBC transfer was reduced in all transplant recipients vs young healthy controls (median [first quartile-third quartile] of 13% [9%-22%] vs 2% [1.75%-3%], p = 0.003) as well as vs age-matched controls (5.5% [2%-9.25%], p = 0.039). Spectroscopy demonstrated reduced RBC/membrane signal (0.26 [0.17-0.31] vs 0.62 [0.50-0.66], $p < 0.001$ and vs 0.48 [0.42-0.55], p = 0.002), reduced RBC chemical shift (217.4 [217.2-217.7] ppm vs 218.2 [218.0-218.5] ppm, p = 0.009 and vs 218.3 [218.2-218.5] ppm, p = 0.003), and increased RBC oscillation amplitude vs the young healthy controls (14.1% [12.2%-16.4%] vs 11.1% [9.9%-11.9%], p = 0.003).

CONCLUSIONS: Patients with CLAD exhibited significant ventilation defects that correlated with FEV_1 decline, which, along with RBC transfer defects and other ^{129}Xe gas-exchange and hemodynamic

*Corresponding author: Department of Medicine, Duke University, Durham, NC.
E-mail address: hakim.azfarali@duke.edu.

2950-1334/© Published by Elsevier Inc. on behalf of International Society for Heart and Lung Transplantation. This is an open access article under the CC BY-NC-ND license (http://creativecommons.org/licenses/by-nc-nd/4.0/).
https://doi.org/10.1016/j.jhlto.2024.100117

abnormalities, could provide a promising means of early detection of physiological changes in patients with CLAD.

JHLT Open 2024;5:100117

© Published by Elsevier Inc. on behalf of International Society for Heart and Lung Transplantation. This is an open access article under the CC BY-NC-ND license (http://creativecommons.org/licenses/by-nc-nd/4.0/).

Background

Chronic lung allograft dysfunction (CLAD) is the leading cause of long-term mortality in lung transplant recipients and is of paramount concern for clinicians.[1] As there is currently no effective treatment to reverse established CLAD, early detection is of the utmost importance to slow or stop disease progression.[2] However, despite its implications for long-term patient outcomes, we still lack early detection methods that can accurately and noninvasively screen for CLAD.[3]

CLAD has been described as presenting with several heterogeneous phenotypes, predominantly bronchiolitis obliterans syndrome (BOS), restrictive allograft syndrome, and mixed phenotypes.[4] Individual CLAD phenotypes display unique clinical presentations, have distinct patterns on pulmonary function testing (PFT), radiographs, and computed tomography (CT) scans, and exhibit dissimilar responsiveness to therapies. Despite these phenotypic differences, other important diagnostic and prognostic criteria, such as early detection, staging, and treatment management, remain a challenge. To this end, the International Society for Heart and Lung Transplantation (ISHLT) released a consensus report in 2019 seeking to standardize the approach to CLAD identification and treatment. Although the ISHLT report has done much to harmonize diagnostic criteria, there remains room for provider subjectivity as CLAD remains a clinical diagnosis based on arbitrary PFT decline thresholds. Furthermore, based on the advised diagnostic criteria, the current methodology may lead to instances of delayed diagnosis.[5,6]

Several approaches to the detection of CLAD exist but do not show significant promise as they often fail to make a definitive diagnosis early in the disease course.[3,7] PFTs currently constitute the standard of care for initial diagnosis of CLAD, after exclusion of reversible causes of allograft dysfunction, followed by monitoring of patients over time. The ISHLT highlighted this connection in their previous consensus report, defining CLAD as a persistent decline in forced expiratory volume in 1 second (FEV_1) (≥ 20%) compared to a reference value obtained from 2 maximal post-transplant FEV_1 values obtained at least 3 weeks apart.[4] However, determining whether an observed decline in PFTs is a result of CLAD rather than a manifestation of a concurrent illness remains the purview of the overseeing physician.[4] Reliance on PFTs alone is additionally problematic since accuracy and repeatability are often difficult to achieve in frail patient populations.[7] Furthermore, PFTs provide information on global airway function rather than regional ventilation heterogeneity, and thus PFT detection of CLAD only occurs after significant and irreversible damage is already present.[8] Therefore, PFTs are often paired with imaging modalities that can detect regional changes in ventilation physiology.

The most common imaging modality used in managing patients with CLAD is CT, which is frequently ordered following an initial decline in FEV_1 that leads to clinical suspicion of possible CLAD.[3] CT imaging enables the differentiation between CLAD and non–CLAD-related abnormalities in pulmonary function, such as infection or airway stenosis. In addition, CT imaging enables the delineation of CLAD phenotypes through detection of bronchial wall thickening and expiratory air trapping, as seen with obstructive phenotypes, or by the identification of subpleural thickening and ground-glass opacities, as seen with restrictive phenotypes.[9] CT is often central to determining the severity of lung involvement and to discussions surrounding CLAD prognosis and treatment. Although it has many advantages, CT sensitivity for the early detection of CLAD ranges from 25% to 88% depending on the criteria used.[9–11] This is partly attributed to overestimating or underestimating airflow obstruction in the absence of other indices, such as spirometry.[9] Furthermore, radiation exposure is of particular concern for immunodeficient patient populations and, given that this modality provides a primarily structural assessment, pulmonary function decline must often be inferred.[8,12]

An evolving imaging approach is magnetic resonance imaging (MRI) using hyperpolarized gases such as ^{3}He and ^{129}Xe. This modality provides a noninvasive means to image the 3-dimensional ventilation distribution of these inhaled gases in a single breath hold. This approach confers a high level of sensitivity to detecting regional hypoventilation because imaging reveals the functional boundaries of the lung, thereby facilitating detection of small peripheral defects.[13,14] Thus, even imaging at a single time point can reveal ventilation abnormalities that may indicate early obstruction. This technology was applied using ^{3}He MRI early in the development of the field, which demonstrated its sensitivity for the early detection of CLAD in single-lung transplant recipients.[15] Furthermore, the absence of ionizing radiation in ^{3}He MRI permitted it to be used for serial monitoring.[8] More recently, due to supply limitations of ^{3}He, hyperpolarized ^{129}Xe gas has emerged as the primary hyperpolarized gas for regional assessment of pulmonary function.[16]

Notably, MRI with ^{129}Xe gas allows for not only the visualization of pulmonary ventilation, but through its solubility and distinct frequency shifts, permits imaging of gas uptake into the interstitial membrane tissues and transfer to the capillary red blood cells (RBC).[17] This 3-compartment

imaging technique provides a means to estimate and visualize each of the components of gas exchange as measured by the diffusing capacity of carbon monoxide—accessible alveolar volume, membrane conductance, and capillary blood volume.[18] Moreover, in the same 15- to 20-minute exam, ^{129}Xe spectroscopy can reveal average capillary blood oxygenation of the RBCs and oscillations in the RBC signal amplitude that speak to the presence of pulmonary hypertension.[19] However, the use of hyperpolarized ^{129}Xe functional imaging and spectroscopy has not yet been investigated in lung transplant populations. In this study, we sought to characterize the patterns of ^{129}Xe ventilation, gas exchange, and spectroscopy in patients with CLAD and establish correlations with staging.

Materials and methods

Patient recruitment and characteristics

The study was approved by an Institutional Review Board and recruited a cohort of 10 patients with a medical history of bilateral lung transplantation. Their findings were compared to a cohort of 16 young healthy control volunteers and 16 age-matched healthy control volunteers with no history of pulmonary disease who had undergone identical scanning previously. Written informed consent was obtained from each participant before study recruitment and patients underwent ^{129}Xe MRI between 2017 and 2022. Hyperpolarized ^{129}Xe was produced and dispensed under an investigational new drug application (no. 109,490). All participants were over 18 years of age. One patient was found to have a lung infection at the time of imaging and was removed from the analysis cohort due to its confounding effects. Of the 9 transplant recipients analyzed, the mean age was 63 ± 12 years and the mean time from transplant was 103 ± 82 months. The mean ages of the young healthy control and age-matched healthy control volunteers were 25 ± 3 years and 63 ± 9 years, respectively. All lung transplant subjects were screened for CLAD based on PFTs utilizing the ISHLT criteria in clinical collaboration with providers at our center. Within our remaining lung transplant patient cohort (n = 9), 7 subjects demonstrated spirometry values indicative of CLAD, and 2 subjects did not.

^{129}Xe polarization and dose administration

^{129}Xe (86% isotopically enriched, Linde Gases) was hyperpolarized by spin-exchange optical pumping and cryogenically accumulated using a commercially available polarizers (Models 9820 and 9810, Polarean) before allocation into a Tedlar dose delivery bag (Jensen Inert Products), as previously described.[20] Hyperpolarized ^{129}Xe imaging and spectroscopy were conducted on a 3.0-T scanner (Siemens Magnetom Trio VB19A and Prisma XA30A). Subjects were fitted with a flexible vest coil (Clinical MR Solutions) and received 2 separate doses of ^{129}Xe, 1 for calibration/spectroscopy, and 1 for ^{129}Xe gas-exchange MRI. For the calibration/spectroscopy scans, subjects received a mean ± SD ^{129}Xe dose equivalent of 78.0 ± 19.3 ml. (The dose equivalent represents the net magnetization that would be obtained from a similar volume of 100% polarized, 100% enriched ^{129}Xe.) For gas-exchange MRI, a larger dose equivalent of 160.0 ± 51.9 ml was administered. Xenon volumes ranged between 300 and 875 ml depending on the type of acquisition and were buffered with a nonpolarized ^{129}Xe blend to fully inflate the dose delivery bag. For 23 of 41 subjects, the total dose volume was selected to be 500, 750, or 1000 ml in volume based on 20% of the patient's forced vital capacity and was inhaled from functional residual capacity. The remaining 18 subjects received 1-liter untailored dose volumes (specifically: 3 of 9 transplant subjects, 9 of 16 young healthy subjects, and 6 of 16 age-matched healthy subjects). One subject required supplemental oxygen during MRI, which was administered by nasal cannula and removed 2 breaths before ^{129}Xe inhalation. Patient vitals (heart rate and arterial oxygen saturation) were monitored continuously using an MRI-compatible monitoring system (Model 7500, Nonin). Participants underwent ^{129}Xe gas-exchange MRI during a 15-second breath hold. The combined calibration and spectroscopy scan was performed during an 8-second breath hold and acquired 500 ^{129}Xe free-induction decays at 15-msec intervals (echo time, 0.45 msec; target flip angle, 20°; dwell time, 20 μsec; 512 points).[21] Three-dimensional images were obtained during the breath hold using an interleaved radial acquisition of gas- and dissolved-phase (i.e., membrane uptake and RBC signals). Dissolved-phase images were obtained with an effective repetition time of 15 msec and flip angle of 20° and an echo time that allowed the dissolved-phase compartments to be decomposed using the 1-point Dixon method.[22] This process generated 3-dimensional images of the gas, membrane uptake, and RBC components with a nominal isotropic resolution of 6.3 mm.

Image processing and analysis

Quantitative analysis of pulmonary ventilation, membrane uptake, and transfer to RBC compartments was performed according to previously published methods.[18] Briefly, ventilation scans were transformed into quantitative maps after normalizing by the top percentile of intensities and mapping the histogram into 6 classification bins using reference thresholds from a healthy reference population.[13] These maps were color-coded in increments of 1 standard deviation away from the healthy reference mean and were quantified according to the voxels at least 2 standard deviations below the healthy reference mean (the "ventilation defect percent," or VDP). Similarly, membrane uptake and RBC transfer were rendered into quantitative maps by dividing by the gas-phase signal on a voxel-by-voxel basis and similarly color-coded in increments of 1 standard deviation from the reference mean. Membrane maps were quantified according to the membrane high percentage or MHP (at least 2 standard deviations above the healthy reference mean) and membrane defect percent or MDP (at least 2 standard deviations below). RBC transfer maps were quantified according to the RBC transfer defect percent or (at least 2 standard deviations below the healthy

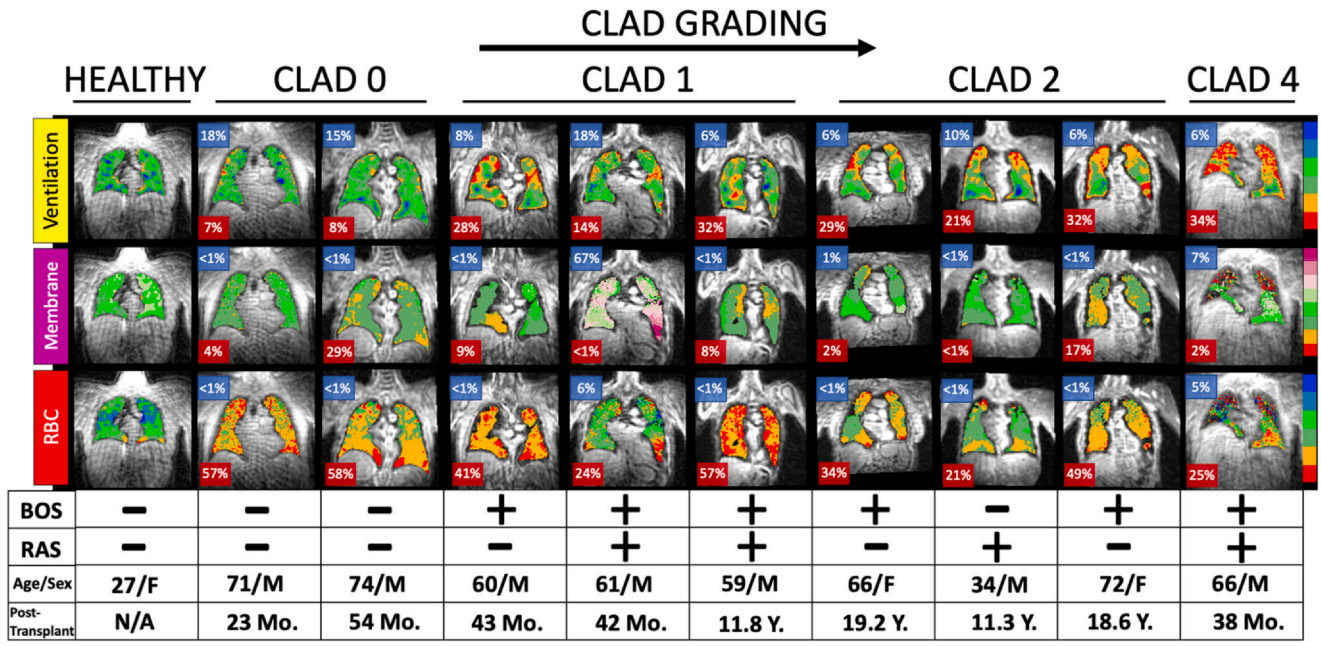

BOS	−	−	−	+	+	+	+	−	+	+
RAS	−	−	−	−	+	+	−	+	−	+
Age/Sex	27/F	71/M	74/M	60/M	61/M	59/M	66/F	34/M	72/F	66/M
Post-Transplant	N/A	23 Mo.	54 Mo.	43 Mo.	42 Mo.	11.8 Y.	19.2 Y.	11.3 Y.	18.6 Y.	38 Mo.

Figure 1 ^{129}Xe magnetic resonance imaging (MRI) maps of ventilation, hemoglobin-corrected membrane uptake, and red blood cell (RBC) transfer from an example young healthy subject and 9 lung allograft subjects. For each ventilation, membrane uptake, and RBC map, the lowest of the color bins corresponds to the VDP, MDP, and RDP, respectively. The membrane has the additional MHP value corresponding to voxels more than 2 standard deviations above reference mean. Corresponding abnormalities varied widely across the population. CLAD grading was based on PFT values. All maps are overlaid onto an anatomical proton MRI scan for reference. The black areas on the membrane and RBC maps are associated with regions of ventilation defect where further quantitative analysis is not possible. BOS, bronchiolitis obliterans syndrome; CLAD, chronic lung allograft dysfunction; MDP, membrane defect percent; RAS, restrictive allograft syndrome; RDP, red blood cell transfer defect percent; VDP, ventilation defect percent.

reference mean). Given that transplant patients receiving immunosuppressive therapy may have decreased hemoglobin, all gas-exchange images in the cohort were corrected for hemoglobin to a standardized value of 14 g/dl according to the recently published equations.[23]

Spectroscopy processing and analysis

Free-induction decays were fit to gas, membrane uptake, and RBC transfer peaks in the time domain with each peak described by an amplitude, chemical shift, phase, and full width at half maximum.[21] Calculated indices included the RBC/membrane ratio, RBC static chemical shift, and RBC oscillation amplitude.

Pulmonary function tests

Spirometry was obtained using functional tests that met the technical criteria set by the American Thoracic Society and European Respiratory Society and compiled retrospectively from patient chart reviews.[24,25]

CT imaging

Representative CT scans of Transplant Subjects were retrieved retrospectively from within a 6-month window of the ^{129}Xe MRI. The description of specific CT findings was summarized from interpretations made by board-certified radiologists from the affiliated hospital system.

Statistical analysis

Pairwise Wilcoxon rank-sum tests (i.e., separate comparisons between pairs of groups) were used to analyze the differences between the healthy and lung transplant groups. All the Wilcoxon rank-sum tests were evaluated with a statistical significance threshold of $p < 0.05$, using the Holm-Bonferroni correction for multiple comparisons. Correlations with clinical metrics were assessed using the Spearman correlation with a statistical significance level of $p < 0.05$. Statistical analysis was performed with R software (version 3.6.0, R Foundation for Statistical Computing).

Results

Representative ^{129}Xe MRI findings

CLAD designations were adjudicated and graded by transplant physicians based on ISHLT guidelines.[4] Seven lung allograft subjects demonstrated PFT values consistent with a diagnosis of CLAD, while 2 did not and thus were designated as CLAD 0. Among the 7 subjects with CLAD, additional grading was assigned based on the severity of spirometry scoring, namely grade 1 ($n = 3$), grade 2 ($n = 3$), and grade 4 ($n = 1$). All patients tolerated the ^{129}Xe MRI without incident. Figure 1 shows images of ventilation, membrane uptake, and RBC transfer from the 9 lung allograft subjects. All subjects demonstrated areas of

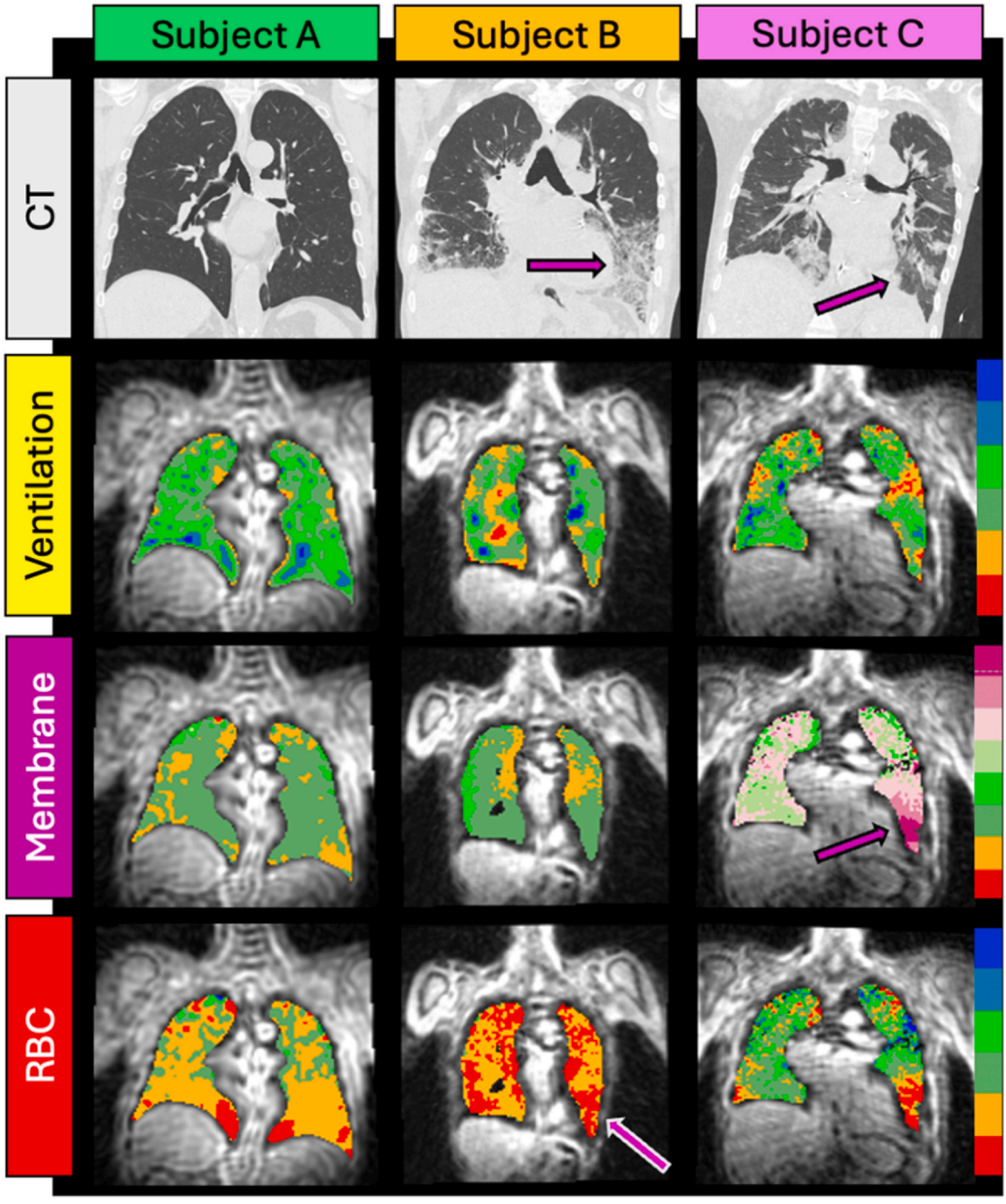

Figure 2 CT and ^{129}Xe gas-exchange maps of 3 lung allograft subjects. Subject A (CLAD 0) demonstrates normal appearing CT, with no evidence to suggest BOS. However, RBC transfer is markedly reduced. Subject B (CLAD 1) demonstrates bilateral mid and lower lung predominant diffuse ground-glass and consolidative opacities on CT. This subject exhibits modest ventilation defects, but markedly reduced RBC transfer on ^{129}Xe MRI. Subject C (CLAD 1) exhibits multifocal bilateral peribronchovascular ground-glass patterns on CT, with regions of mild confluent consolidation and associated intra- and interlobular septal thickening ("crazy paving"). This patient exhibits high membrane uptake and poor RBC transfer in the lower left lung that associates with ground-glass/consolidations, in addition to areas of high membrane that correspond to relatively normal-looking regions of CT. This pattern of high membrane uptake with otherwise preserved RBC transfer may suggest "early stage" allograft rejection. BOS, bronchiolitis obliterans syndrome; CLAD, chronic lung allograft dysfunction; CT, computed tomography; MRI, magnetic resonance imaging; RBC, red blood cell.

ventilation defect (red) and low ventilation (yellow), and these deficiencies were especially prominent in CLAD 1 to 4 cohorts. Several CLAD 1 to 4 subjects also exhibited regions of reduced membrane uptake (red and yellow) and all lung allograft subjects exhibited areas of low RBC transfer irrespective of CLAD phenotype. Note that in the membrane and RBC maps, dark areas within the thoracic cavity represent unventilated regions (defects) where analysis of gas exchange is not possible. Corresponding CT scans acquired from a subset of 3 subjects are shown in Figure 2. Note, in particular, the reduced RBC transfer in the absence of CT abnormalities (subject A) as well as

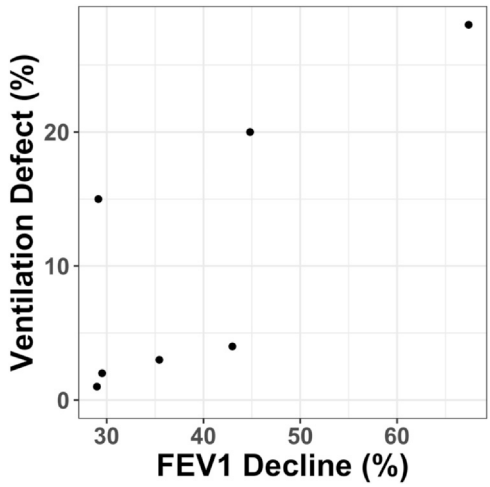

Figure 3 Correlation between percentage decline in FEV_1 from its maximal post-transplant value and ventilation defect percent (VDP) derived from ^{129}Xe MRI in chronic lung allograft subjects. The ^{129}Xe VDP seen in established CLAD patients (grade I or greater) was significantly correlated with the severity based on FEV_1 decline (rho = 0.79, $p = 0.048$). CLAD, chronic lung allograft dysfunction; FEV_1, forced expiratory volume in 1 second.

reduced RBC transfer in the presence of clear fibrotic activity (subject B). Notably, subject C has increased membrane signal in both regions of CT abnormality and regions where the CT is relatively normal; coupled with the largely preserved RBC transfer in this subject, this combination may suggest early stages of disease activity presaging further CT involvement and vascular abnormalities.

Correlations between FEV_1 decline and ^{129}Xe ventilation indices

Figure 3 shows the correlation between percentage decrease in FEV_1 from its maximum post-transplant value and VDP derived from ^{129}Xe MRI, excluding CLAD 0 patients who, by definition, did not exhibit FEV_1 decline. The decline in FEV_1 was significantly correlated with VDP measured on ^{129}Xe MRI (rho = 0.79, $p = 0.048$). Notably, this analysis included all CLAD subjects, regardless of phenotype, and thus certain pathologies may have skewed measured relationships between FEV_1 and VDP variables.

^{129}Xe gas-exchange MRI findings

^{129}Xe gas-exchange patterns were compared between healthy control ($n = 16$), healthy age-matched ($n = 16$), and lung allograft participants ($n = 9$) as shown in Figure 4. VDP was significantly higher in lung allograft subjects (median [first quartile-third quartile] of 3% [1%-15%]) than in young healthy control participants (0% [0%-1%], $p = 0.002$) and age-matched healthy controls (1% [0.75%-1%], $p = 0.026$), as was hemoglobin-corrected RDP, which was 13% [9%-22%] in the lung allograft subjects vs 2% [1.75%-3%] in the young healthy controls ($p = 0.003$) and 5.5% [2%-9.25%] in the age-matched controls ($p = 0.039$). There was no difference in MHP or MDP across all 3 populations.

^{129}Xe spectroscopy

Figure 5 compares RBC/membrane ratio, RBC chemical shift, and RBC oscillation amplitude in healthy controls and participants with lung allografts. The hemoglobin-corrected RBC/membrane ratio was significantly lower in participants with lung allografts (0.26 [0.17-0.31]) than in young healthy control participants (0.62 [0.50-0.66]; $p < 0.001$) and age-matched healthy controls (0.48 [0.42-0.55], $p = 0.002$). RBC chemical shift was significantly lower in lung allograft subjects (217.4 [217.2-217.7] ppm compared to young healthy controls (218.2 [218.0-218.5] ppm, $p = 0.009$) and age-matched controls (218.3 [218.2-218.5] ppm, $p = 0.003$). RBC oscillation amplitude was also higher in lung allograft subjects (14.1% [12.2%-16.4%]) than in young healthy controls (11.1% [9.9%-11.9%], $p = 0.003$) and on the cusp of significance vs age-matched controls (11.9% [10.7%-13.5%], $p = 0.054$).

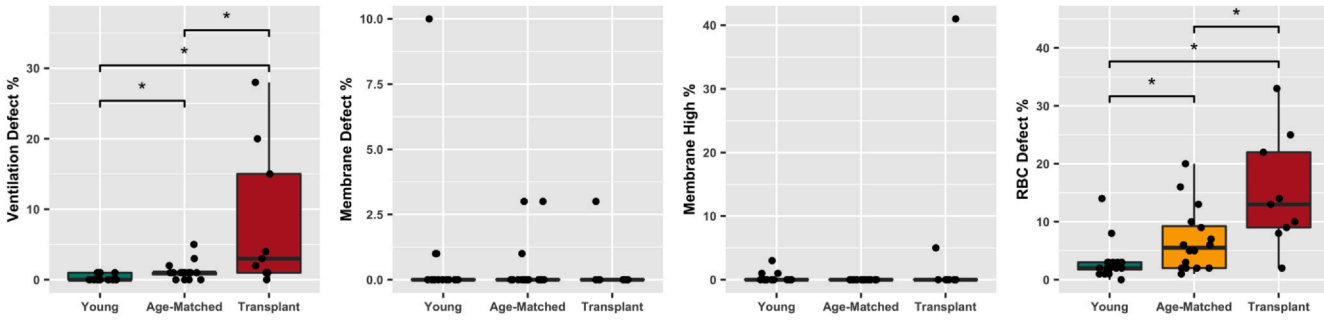

Figure 4 Box plots showing metrics derived from ^{129}Xe ventilation (ventilation defect percent (VDP), membrane high and membrane defect percent (MHP and MDP), and RBC transfer defect percent (RDP) in healthy control participants and participants with lung allografts. Horizontal solid lines are first quartile, median, and third quartile. VDP (far left) was significantly higher in lung allograft subjects (median [first quartile-third quartile] of 3% [1%-15%]) than in young healthy control participants (0% [0%-1%], $p = 0.002$) and age-matched healthy controls (1% [0.75%-1%], $p = 0.026$), as was hemoglobin-corrected RDP, which was 13% [9%-22%] in the lung allograft subjects vs 2% [1.75%-3%] in the young healthy controls ($p = 0.003$) and 5.5% [2%-9.25%] in the age-matched controls ($p = 0.039$). There was no difference in MHP or MDP across all 3 populations. RBC, red blood cells.

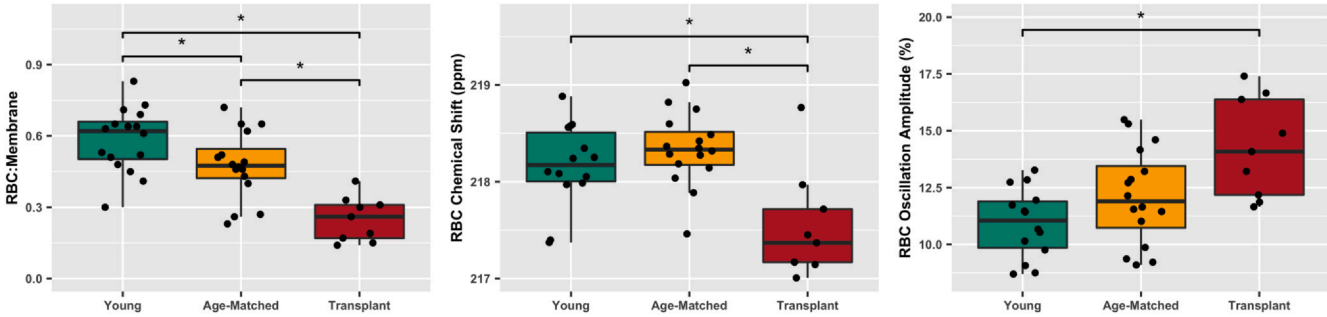

Figure 5 Top row: box plots comparing ^{129}Xe MR spectroscopy measurement between healthy control participants and those with lung allografts. The hemoglobin-corrected RBC: membrane ratio (left) was significantly lower in participants with lung allografts (0.26 [0.17-0.31]) than in young healthy control participants (0.62 [0.50-0.66]; $p < 0.001$) and age-matched healthy controls (0.48 [0.42-0.55], $p = 0.002$). RBC chemical shift was significantly lower in lung allograft subjects (217.4 [217.2-217.7] ppm compared to young healthy controls (218.2 [218.0-218.5] ppm, $p = 0.009$) and age-matched controls (218.3 [218.2-218.5] ppm, $p = 0.003$). RBC oscillation amplitude was also higher in lung allograft subjects (14.1% [12.2%-16.4%]) than in young healthy controls (11.1% [9.9%-11.9%], $p = 0.003$) and on the cusp of significance vs age-matched controls (11.9% [10.7%-13.5%], $p = 0.054$). MR, magnetic resonance; RBC, red blood cells.

Discussion

In this study, we found that CLAD subjects exhibited significant ventilation defects on ^{129}Xe MRI compared to healthy volunteers. In CLAD patients, grade 1 and above ^{129}Xe VDP was correlated with the percentage decline in FEV_1 from maximum post-transplant value. One advantage of the VDP metric is that it is independent of traditional reference values required for PFTs. As VDP is always evaluated relative to the patient's lung volume measured on imaging, it is sensitive to early obstructive changes and may be used as an objective measure of regional ventilation abnormalities at any time point. While the relationship between ^{129}Xe MRI and FEV_1 decline may be more complicated than what is captured by linear regression, this approach provided assurance that VDP does correlate to some extent with this common metric of interest.

Even after Hemoglobin correction, we observed significantly increased RBC transfer defects in the transplant cohort (including 2 with CLAD 0) relative to healthy controls. Although these 2 subjects exhibited minimal ventilation abnormalities, they both had significant RBC transfer defects, suggesting this may be an important marker of early allograft dysfunction predating ventilation defects. RBC transfer defects have been a consistent finding in a wide range of lung diseases, including interstitial lung diseases such as idiopathic pulmonary fibrosis (IPF), nonspecific interstitial pneumonia (NSIP), and chronic hypersensitivity pneumonitis (cHP), as well as chronic obstructive pulmonary disease (COPD) and pulmonary vascular disease.[26,27] While minor RBC transfer defects are also a feature of normal aging,[28] injury to the vascular bed during the transplantation process is conceivable, and the possibility of transient lung ischemia injury resulting in deleterious effects on the pulmonary endothelium post-transplantation cannot be ignored.[29] RBC transfer defects are thought to be associated with occlusion, vasoconstriction, or loss of pulmonary capillary microvasculature. There have been several recent studies offering possible explanations as to the relationship between CLAD phenotypes and pulmonary microvascular changes. One such study suggests a correlation between patients with restrictive lung allograft dysfunction and smaller vascular volumes.[30] Another study points to vascular changes seen on histology on up to 44% of BOS, and even emphysematous changes, possibly offering insight as to the low membrane uptake seen in a number of our patients, a feature more typical of COPD.[31,32]

The finding of high membrane uptake (MHP = 60%) in 1 subject with a mixed BOS/restrictive allograft syndrome phenotype was particularly intriguing. High membrane uptake is increasingly recognized to be associated with interstitial lung diseases, such as IPF, NSIP, cHP, and progressive pulmonary fibrosis in general.[26,27] While obviously not statistically significant in this sample, this is the feature one might speculate would most likely be associated with restrictive allograft dysfunction.

The ^{129}Xe MR spectroscopy findings in our transplant cohort reflected features of impaired gas exchange, particularly the reduced RBC/membrane ratio and reduced RBC chemical shift. The median Hb-corrected RBC/membrane ratio in allograft subjects was half that of healthy volunteers, suggesting substantial gas-exchange impairment in this cohort and consistent with the RBC transfer defects seen on imaging. Similarly, the RBC chemical shift was reduced in the transplant patients. This metric is thought to reflect mean capillary blood oxygenation levels and suggests a reduced transit time through the microvasculature, and it is also consistent with RBC transfer defects seen on imaging. This was similarly reflected in RBC oscillation amplitudes that were enhanced in the transplant cohort. This metric is thought to reflect cardiogenic oscillations in microvascular flow rates and, again, with the reduced capillary bed suggested by RBC transfer defects, indicates higher overall flow and shorter transit times.

We recognize there were several limitations within this study, particularly the small sample size and inclusion of only bilateral recipients. Our CLAD cohort had a predominance of the more common BOS phenotype. A wider sample of both phenotype and grade should be included in

future studies. Such studies should also consider longitudinal monitoring of ^{129}Xe gas-exchange metrics post-transplant to evaluate the sequential changes in gas exchange, spectroscopy, and ventilation defects during CLAD development, as well as investigating observed differences in gas-exchange function in patients with earlier interventions. Particularly, it would be useful to obtain images of lung transplant recipients near their peak pulmonary function, which would provide useful context by which to interpret the images of the CLAD 0 patients.

Conclusion

These preliminary results suggest that hyperpolarized ^{129}Xe MRI and spectroscopy may be used to elucidate early detection of airway obstruction and RBC transfer defects in patients with CLAD. Future studies focused on ^{129}Xe MRI characteristics early in the disease course will advance this work and will further explore its clinical impact.

Author contributions

Guarantor of integrity of entire study, A.A.; study concepts/study design or data acquisition or data analysis/interpretation, all authors; manuscript drafting or manuscript revision for important intellectual content, all authors; approval of final version of submitted manuscript, all authors; agrees to ensure any questions related to the work are appropriately resolved, all authors; literature research, A.S., S.P., B.D., A.A.; clinical studies, S.P., B.D., A.A.; statistical analysis, D.M., S.Z., S.L.; and manuscript editing, A.S., D.M., S.P., B.D., A.A.

Disclosure statement

The authors declare the following financial interests/personal relationships which may be considered as potential competing interests: Dr Bastiaan Driehuys reports financial support was provided by the National Institutes of Health. Dr Bastiaan Driehuys reports a relationship with Polarean Imaging that includes board membership and equity or stocks. Dr David Mummy reports a relationship with Polarean Imaging that includes consulting or advisory. Scott M. Palmer reports a relationship with Incyte Corporation that includes funding grants. Scott M. Palmer reports a relationship with AstraZeneca that includes funding grants. Scott M. Palmer reports a relationship with Bristol-Myers Squibb that includes funding grants and speaking and lecture fees. Scott M. Palmer reports a relationship with CareDx Inc. that includes funding grants. Scott M. Palmer reports a relationship with Boehringer Ingelheim Pharmaceuticals Inc. that includes funding grants and speaking and lecture fees. Scott M. Palmer reports a relationship with UpToDate that includes equity or stocks. Scott M. Palmer reports a relationship with Altavant Sciences that includes speaking and lecture fees. The other authors declare that they have no known competing financial interests or personal relationships that could have appeared to influence the work reported in this paper.

Duke Radiology Seed Funds, NIH/NHLBI R01HL105643, R01HL12677.

References

1. Opelz G, Döhler B, Ruhenstroth A, et al. The collaborative transplant study registry. Transplant Rev 2013;27:43-5. https://doi.org/10.1016/j.trre.2013.01.004.
2. Tissot A, Danger R, Claustre J, Magnan A, Brouard S. Early identification of chronic lung allograft dysfunction: the need of biomarkers. Front Immunol 2019;10:e1681. https://doi.org/10.3389/fimmu.2019.01681.
3. Tian D, Huang H, Wen HY. Noninvasive methods for detection of chronic lung allograft dysfunction in lung transplantation. Transplant Rev 2020;34:e100547. https://doi.org/10.1016/j.trre.2020.100547.
4. Verleden GM, Glanville AR, Lease ED, et al. Chronic lung allograft dysfunction: Definition, diagnostic criteria, and approaches to treatment——a consensus report from the Pulmonary Council of the ISHLT. J Heart Lung Transplant 2019;38:493-503. https://doi.org/10.1016/j.healun.2019.03.009.
5. Levy L, Huszti E, Renaud-Picard B, et al. Risk assessment of chronic lung allograft dysfunction phenotypes: validation and proposed refinement of the 2019 International Society for Heart and Lung Transplantation classification system. J Heart Lung Transplant 2020;39:761-70. https://doi.org/10.1016/j.healun.2020.04.012.
6. Berra G, Huszti E, Levy L, et al. Phenotyping CLAD after single lung transplant: limits and prognostic assessment of the 2019 ISHLT classification system. J Heart Lung Transplant 2022;41:599-607. https://doi.org/10.1016/j.healun.2022.01.015.
7. Enright PL, Beck KC, Sherrill DL. Repeatability of spirometry in 18,000 adult patients. Am J Respir Crit Care Med 2004;169:235-8. https://doi.org/10.1164/rccm.200204-347OC.
8. Pennati F, Salito C, Borzani I, et al. Quantitative multivolume proton-magnetic resonance imaging in lung transplant recipients: comparison with computed tomography and spirometry. Acad Radiol 2021;28:e297-305. https://doi.org/10.1016/j.acra.2020.05.026.
9. Byrne D, Nador RG, English JC, et al. Chronic lung allograft dysfunction: review of ct and pathologic findings. Radiol Cardiothorac Imaging 2021;3:e200314. https://doi.org/10.1148/ryct.2021200314.
10. Hota P, Dass C, Kumaran M, Simpson S. High-resolution ct findings of obstructive and restrictive phenotypes of chronic lung allograft dysfunction: more than just bronchiolitis obliterans syndrome. Am J Roentgenol 2018;211:W13-21. https://doi.org/10.2214/AJR.17.19041.
11. Brun AL, Chabi ML, Picard C, Mellot F, Grenier PA. Lung transplantation: Ct assessment of chronic lung allograft dysfunction (CLAD). Diagnostics 2021;11:e817. https://doi.org/10.3390/diagnostics11050817.
12. Voskrebenzev A, Greer M, Gutberlet M, et al. Detection of chronic lung allograft dysfunction using ventilation-weighted Fourier decomposition MRI. Am J Transplant 2018;18:2050-60. https://doi.org/10.1111/ajt.14759.
13. He M, Driehuys B, Que LG, Huang YCT. Using hyperpolarized ^{129}Xe MRI to quantify the pulmonary ventilation distribution. Acad Radiol 2016;23:1521-31. https://doi.org/10.1016/j.acra.2016.07.014.
14. He M, Kaushik SS, Robertson SH, et al. Extending semiautomatic ventilation defect analysis for hyperpolarized ^{129}Xe ventilation MRI. Acad Radiol 2014;21:1530-41. https://doi.org/10.1016/j.acra.2014.07.017.
15. Gast KK, Zaporozhan J, Ley S, et al. ^{3}He-MRI in follow-up of lung transplant recipients. Eur Radiol 2004;14:78-85. https://doi.org/10.1007/s00330-003-2092-4.
16. Walkup LL, Myers K, El-Bietar J, et al. Xenon-129 MRI detects ventilation deficits in paediatric stem cell transplant patients unable to perform spirometry. Eur Respir J 2019;53:e1801779. https://doi.org/10.1183/13993003.01779-2018.

17. Mummy DG, Coleman EM, Wang Z, et al. Regional gas exchange measured by ^{129}Xe magnetic resonance imaging before and after combination bronchodilators treatment in chronic obstructive pulmonary disease. J Magn Reson Imaging 2021;54:964-74. https://doi.org/10.1002/jmri.27662.
18. Wang JM, Robertson SH, Wang Z, et al. Using hyperpolarized ^{129}Xe MRI to quantify regional gas transfer in idiopathic pulmonary fibrosis. Thorax 2018;73:21-8. https://doi.org/10.1136/thoraxjnl-2017-210070.
19. Bier EA, Alenezi F, Lu J, et al. Noninvasive diagnosis of pulmonary hypertension with hyperpolarised ^{129}Xe magnetic resonance imaging and spectroscopy. ERJ Open Res 2022;8:e00035. https://doi.org/10.1183/23120541.00035-2022.
20. He M, Robertson SH, Kaushik SS, et al. Dose and pulse sequence considerations for hyperpolarized ^{129}Xe ventilation MRI. Magn Reson Imaging 2015;33:877-85. https://doi.org/10.1016/j.mri.2015.04.005.
21. Bier EA, Robertson SH, Schrank GM, et al. A protocol for quantifying cardiogenic oscillations in dynamic ^{129}Xe gas exchange spectroscopy: the effects of idiopathic pulmonary fibrosis. NMR Biomed 2019;32:e4029. https://doi.org/10.1002/nbm.4029.
22. Kaushik SS, Robertson SH, Freeman MS, et al. Single-breath clinical imaging of hyperpolarized ^{129}Xe in the airspaces, barrier, and red blood cells using an interleaved 3D radial 1-point Dixon acquisition. Magn Reson Med 2016;75:1434-43. https://doi.org/10.1002/mrm.25675.
23. Bechtel A, Lu J, Mummy D, et al. Establishing a hemoglobin adjustment for ^{129}Xe gas exchange MRI and MRS. Magn Reson Med 2023;90:1555-68. https://doi.org/10.1002/mrm.29712.
24. Wanger J, Clausen JL, Coates A, et al. Standardisation of the measurement of lung volumes. Eur Respir J 2005;26:511-22. https://doi.org/10.1183/09031936.05.00035005.
25. Miller MR, Hankinson J, Brusasco V, et al. Standardisation of spirometry. Eur Respir J 2005;26:319-38. https://doi.org/10.1183/09031936.05.00034805.
26. Mummy DG, Bier EA, Wang Z, et al. Hyperpolarized ^{129}Xe MRI and spectroscopy of gas-exchange abnormalities in nonspecific interstitial pneumonia. Radiology 2021;301:211-20. https://doi.org/10.1148/radiol.2021204149.
27. Wang Z, Bier EA, Swaminathan A, et al. Diverse cardiopulmonary diseases are associated with distinct xenon magnetic resonance imaging signatures. Eur Respir J 2019;54:e1900831. https://doi.org/10.1183/13993003.00831-2019.
28. Mummy D, Zhang S, Bechtel A, et al. Functional gas exchange measures on ^{129}Xe MRI and spectroscopy are associated with age, sex, and BMI in healthy subjects. Front Med 2024;11:e1342499. https://doi.org/10.3389/fmed.2024.1342499.
29. Forgie KA, Fialka N, Freed DH, Nagendran J. Lung transplantation, pulmonary endothelial inflammation, and ex-situ lung perfusion: a review. Cells 2021;10:e1417. https://doi.org/10.3390/cells10061417.
30. Levin K, Lavon B, Muchmore P, Westall G, Snell G. (1222) Identifying imaging biomarkers before the onset of chronic lung allograft dysfunction. J Heart Lung Transplant 2023;42(Suppl 4):S522. https://doi.org/10.1016/j.healun.2023.02.1432.
31. Vanstapel A, Verleden SE, Verbeken EK, et al. Beyond bronchiolitis obliterans: In-depth histopathologic characterization of bronchiolitis obliterans syndrome after lung transplantation. J Clin Med 2022;11:e111. https://doi.org/10.3390/jcm11010111.
32. He M, Qing K, Tustison NJ, et al. Characterizing gas exchange physiology in healthy young electronic-cigarette users with hyperpolarized 129Xe MRI: a pilot study. Int J COPD 2021;16:3183-7. https://doi.org/10.2147/COPD.S324388.